Preparation, Biodistribution and Dosimetry of Copper-64-Labeled Anti-Colorectal Carcinoma Monoclonal Antibody Fragments 1A3-F(ab′)$_2$

Carolyn J. Anderson, Sally W. Schwarz, Judith M. Connett, P. Duffy Cutler, Li Wu Guo, Carl J. Germain, Gordon W. Philpott, Kurt R. Zinn, Douglas P. Greiner, Claude F. Meares and Michael J. Welch

Mallinckrodt Institute of Radiology and Department of Surgery, Washington University School of Medicine, St. Louis, Missouri; University of Missouri Research Reactor, Columbia, Missouri; and Department of Chemistry, University of California, Davis, Davis, California

Antibody fragments labeled with a radiometal using bifunctional chelates generally undergo renal clearance followed by trapping of the metabolites, leading to high radiation doses to the kidneys. Copper-64-labeled BAT-2IT-1A3-F(ab′)$_2$ was recently reported to accumulate in colorectal tumors in an animal model, however, kidney uptake was also high. In this study, the preparation of ^{64}Cu-BAT-2IT-1A3-F(ab′)$_2$ was optimized to reduce the renal uptake. **Methods:** The bifunctional chelate 6-bromoacetamidobenzyl-1,4,8,11-tetraazacyclotetradecane-N,N′,N″,N‴-tetraacetic acid (BAT) was conjugated to 1A3-F(ab′)$_2$ using the linking agent 2-iminothiolane (2IT). The conjugation reaction produced 20% of a lower molecular weight (molecular wieght) impurity found to be TETA-1A3-Fab′. The conjugation procedure was optimized to include FPLC purification of the BAT-2IT-1A3-F(ab′)$_2$ from TETA-1A3-Fab′ after conjugation prior to labeling with ^{64}Cu. The biodistribution of ^{64}Cu-labeled FPLC-purified and unpurified conjugates was determined in normal Sprague-Dawley rats and tumor-bearing Golden Syrian hamsters. Human absorbed doses were calculated from rat biodistribution data and PET imaging of a baboon. **Results:** Upon FPLC purification of the BAT-2IT-1A3-F(ab′)$_2$, the immunoreactivity of ^{64}Cu-labeled 1A3-F(ab′)$_2$ was significantly improved over that of non-FPLC-purified ^{64}Cu-BAT-2IT-1A3-F(ab′)$_2$, and the kidney uptake was decreased in normal rats. The biodistribution in hamsters showed some improvement in both tumor uptake and kidney clearance with FPLC-purified ^{64}Cu-BAT-2IT-1A3-F(ab′)$_2$. **Conclusion:** The improved dosimetry of ^{64}Cu-labeled FPLC purified BAT-2IT-1A3-F(ab′)$_2$ should more readily allow this agent to be investigated clinically to image colorectal cancer using PET.

Key Words: Monoclonal antibody fragments; copper-64; animal biodistribution; dosimetry; colorectal carcinoma

J Nucl Med 1995; 36:850–858

Antibodies labeled with longer-lived, positron-emitting isotopes such as ^{89}Zr ($T_{1/2}$ = 78.4 hr), ^{76}Br ($T_{1/2}$ = 16.1 hr), ^{124}I ($T_{1/2}$ = 4.15 days) and ^{64}Cu ($T_{1/2}$ = 12.8 hr) have advantages over traditionally labeled antibodies due to the improved sensitivity of PET. The anticolorectal carcinoma monoclonal antibody (MAb) 1A3 labeled with the positron-emitting isotope ^{64}Cu was found to be a better agent for detecting small metastases than ^{111}In-labeled MAb 1A3 (*1*). Due to the relatively short half-life of ^{64}Cu (12.8 hr), imaging is performed at 22–24 hr postinjection. In several cases, small metastases (≤1.5 cm) were detected with ^{64}Cu-labeled 1A3 and PET, however, due to the long biological half-life of intact MAbs, the high blood-pool activity remaining at that time presents a problem for image contrast. Along with the disadvantage of a long biological half-life, intact antibodies labeled with radiometals are cleared through the liver and the radiometal is often residualized, making the detection of hepatic metastases difficult. A third disadvantage of the clinical use of radiolabeled intact murine MAbs is the HAMA response. Approximately 50% of people in the ^{64}Cu-labeled 1A3 clinical study developed HAMA (*2*). MAb F(ab′)$_2$ fragments have a shorter biological half-life ($T_{1/2}$ = 12–15 hr), are cleared through both the liver and kidney, and since they do not contain the Fc portion of the MAb, the HAMA formation may be less than with intact MAbs (*3*).

Indium-111-labeled F(ab′)$_2$ fragments have been investigated in both animal models (*4–9*) and in clinical trials (*10–12*). In tumor-bearing nude mice injected with ^{111}In-DTPA-conjugated F(ab′)$_2$ fragments, the blood clearance was relatively rapid compared to radiolabeled intact MAbs, however, the kidney uptake was high (*4,6,7*). In a clinical study of ^{111}In-labeled anti-CEA MAb BW431/31 (*8*), the kidney was the primary critical organ, with an estimated human absorbed dose of 2.27 mGy MBq^{-1}, which was nearly three times higher than the secondary critical organ (testes) with an absorbed dose of 0.8 mGy MBq^{-1}.

The F(ab′)$_2$ fragment of MAb 1A3 has been conjugated to the bifunctional chelate 6-bromoacetamidobenzyl-1,4,8,

Received Mar. 21, 1994; revision accepted Oct. 17, 1994.

For correspondence or reprints contact: Carolyn J. Anderson, PhD, Mallinckrodt Institute of Radiology, 510 S. Kingshighway Blvd. Box 8225, St. Louis, MO 63110.

11-tetraazacyclotetradecane-N,N′,N″,N‴-tetraacetic acid (Br-benzylacetamido-TETA or BAT) and labeled with ^{64}Cu. Biodistribution in normal Sprague-Dawley rats and tumor-bearing hamsters was performed (*13*). The tumor uptake of ^{64}Cu-BAT-2IT-1A3-F(ab′)$_2$ was similar to that of ^{64}Cu-BAT-2IT-1A3, twice as great as ^{125}I-1A3-F(ab′)$_2$ and over three times greater than that of ^{111}In-labeled 1A3-F(ab′)$_2$; however, the radiation dose to the kidney was high, precluding a clinical investigation. We hypothesized that a lower molecular weight impurity present in the ^{64}Cu-labeled 1A3-F(ab′)$_2$ may have been partially responsible for kidney uptake (*13*). In this study, the preparation of the unlabeled conjugate was optimized to eliminate this impurity. The effects of the chromatographic purification of the conjugate and the variation of the chelate-to-MAb ratios on biodistribution in two animal models and immunoreactivity will be discussed. Revised dosimetry estimates were obtained from rat biodistribution data after injection of the ^{64}Cu-BAT-2IT-1A3-F(ab′)$_2$. Human absorbed doses of ^{64}Cu-BAT-2IT-1A3-F(ab′)$_2$ were also determined by PET imaging of a primate and the results will be compared to those obtained from rat biodistribution data.

MATERIALS AND METHODS

All chemicals and methods have been reported previously (*13*) except as listed. Centricon-30 membranes were purchased from Amicon (Beverly, MA). The synthesis of p-nitro-benzyl TETA was performed according to the method of Moi et al. (*14*). Br-benzyl TETA was prepared from nitro-benzyl-TETA as described by McCall et al. (*15*). Centrifuged gel filtration column chromatography was done as reported in the literature (*16*). Radio-thin layer chromatography (radio-TLC) was accomplished using a BIOSCAN System 200 Imaging Scanner (BIOSCAN, Washington, DC). All animal experiments were performed in compliance with guidelines specified by the Washington University Animal Studies Committee and the Jewish Hospital Animal Care Committee.

Preparation and Purification of ^{64}Cu

The procedure for the production of ^{64}Cu at the Missouri University Research Reactor (MURR) has been described in detail elsewhere (*17*). Briefly, zinc metal (99.9999%) was irradiated in the flux trap of the reactor for 150 hr in a boron-nitride-lined container. The fast neutron reaction (n, p) on ^{64}Zn produced ^{64}Cu, while thermal neutron reactions were minimized by the boron-nitride shielding. The procedure to separate the zinc target material from the ^{64}Cu was performed in a sealed glove box. The neutron-irradiated zinc target containing the ^{64}Cu was dissolved in concentrated HCl, and the solution was evaporated to dryness. The chloride salts were dissolved in 1 *M* acetic acid (pH 2.7) and the solution was applied to a disposable Chelex column containing 4–6 ml of resin that was equilibrated with the same acid. Zinc elutes through the Chelex column, whereas the ^{64}Cu remains on the column. The ^{64}Cu was eluted from the Chelex column with 1 *M* HCl. The ^{64}Cu solution (in 1 *M* HCl) was then eluted through a disposable 4–6-ml AG1X8 anion exchange column to remove any remaining zinc. The specific activity of ^{64}Cu was 302 ± 167 Ci/mg Cu (n = 12) at the end of neutron irradiation.

Preparation and Purification of MAbs

MAb 1A3 (intact) was purified from serum-free medium by Invitron (St. Louis, MO) using proprietary methods and 1A3-F(ab′)$_2$ was generated from the intact 1A3 by Invitron through papain digestion followed by column chromatography to separate F(ab′)$_2$ (100 kD) from F$_c$ (31 kD/chain) and any residual intact 1A3 (160 kD). The radiolabeled final product showed no contaminating F$_c$ or intact 1A3. The immunoreactivity (IR) of the antibody fragments generated was determined under conditions of antigen excess (*18*).

Preparation of BAT-2IT-1A3-F(ab′)$_2$ and Labeling with ^{64}Cu

Conjugation of BAT to 1A3-F(ab′)$_2$ was accomplished by previously described methods (*13*). Briefly, a solution of 1A3-F(ab′)$_2$ in 0.1 *M* ammonium phosphate, pH 8, was incubated with excess BAT and freshly prepared 2-iminothiolane (2-IT) in 50 m*M* triethanolamine. Molar ratios of BAT-to-MAb were 20:1, 10:1 or 6:1, and the corresponding molar ratios of 2IT-to-MAb were 10:1, 5:1 or 3:1, respectively. Protein concentrations ranged from 5–10 mg/ml. The solutions were incubated at 37°C for 30 min and purified by gel filtration chromatography using centrifuged columns. One half of each batch of conjugate was further purified by FPLC. Prior to FPLC chromatography, the conjugate was concentrated to 0.2 ml using a Centricon 30 membrane. Approximately 2 mg of conjugate in 0.2 ml buffer was injected onto a Superose 12 size exclusion column eluted at 0.4 ml/min with 0.1 *M* ammonium citrate pH 5.5. The eluate was monitored for UV absorption at 280 nm, and 0.4 ml fractions were collected. The fractions containing the BAT-2IT-1A3-F(ab′)$_2$ (eluting at a retention time corresponding to a molecular weight of 100,000 daltons) were collected and concentrated using Centricon 30 membranes. All chelate-MAb conjugates were stored at −80°C until used. Radiolabeling of BAT-2IT-1A3-F(ab′)$_2$ with ^{64}Cu was carried out at room temperature for 30 min in 0.1 *M* ammonium citrate, pH 5.5 as previously described (*13*).

Isotopic Dilution Assay

The number of chelates conjugated to 1A3-F(ab′)$_2$ at the BAT-to-MAb ratios of 6:1, 10:1 and 20:1 were determined by a modified method of an isotopic dilution assay that has been previously described (*13*). Copper-64-citrate (100 μCi) was added to 10 solutions containing varying amounts of nonradioactive Cu-citrate ranging from 0 to 10 nmole. The "hot plus cold" Cu-citrate was then added to BAT-2IT-1A3-F(ab′)$_2$ (1 nm) and allowed to incubate for 30 min at room temperature. After the 30-min incubation, 1 μmole of EDTA was added to the Cu-labeled antibody fragment conjugates and incubated for 15 min. These solutions were then spotted on silica gel-coated glass plates, developed in 1:1 10% ammonium acetate-to-methanol and analyzed by radio-TLC. Copper-labeled BAT-2IT-1A3-F(ab′)$_2$ remained at the origin, whereas nonspecifically bound $^{64}Cu^{2+}$ bound to EDTA and migrated with an R$_f$ of 0.8. The percent labeling efficiency was plotted as a function of total nanomoles of $^{64}Cu^{2+}$ added to the reaction mixture. The number of chelates attached to the fragment was determined from the inflection point of this curve.

Gel Electrophoresis

In the FPLC purification of BAT-2IT-1A3-F(ab′)$_2$, the 50-kD impurity was collected and concentrated using centricon-30 membranes. Samples were analyzed by sodium dodecyl sulfate, polyacrylamide gel electrophoresis (SDS-PAGE). Approximately 4 μg of sample protein (reduced or unreduced) was applied per lane to

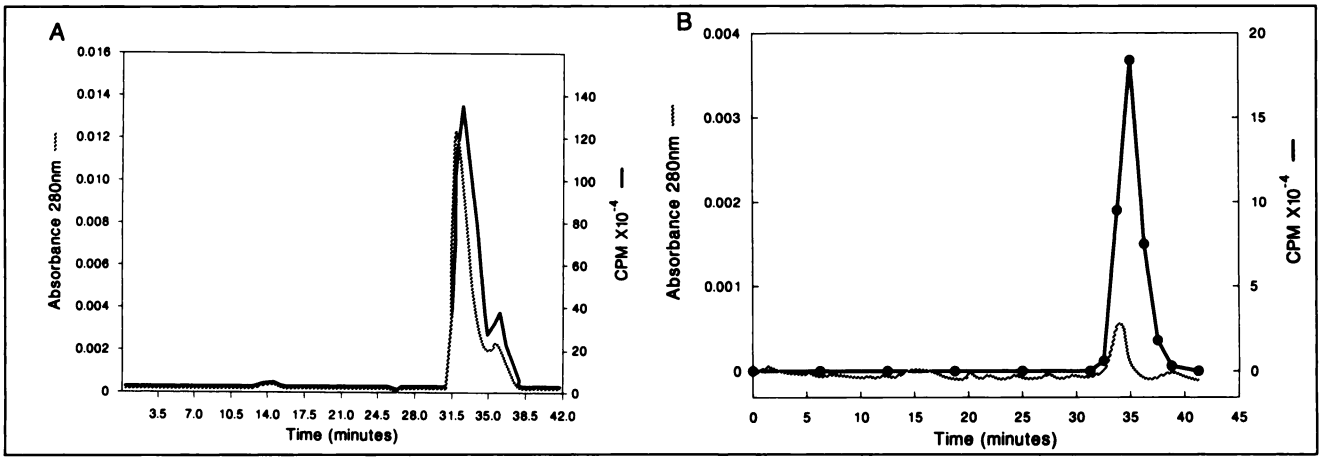

FIGURE 1. (A) FPLC trace of ^{64}Cu-BAT-2IT-1A3-F(ab')$_2$ using unpurified BAT-2IT-1A3-F(ab')$_2$ (20:1 BAT-to-MAb). The column calibration with molecular weight markers indicated that 1A3-F(ab')$_2$ fragment (molecular wieght ~100,000 Da) eluted with a retention time of 32.5 min and the Fab' fragment (molecular wieght ~50,000 Da) eluted with a time of 36.0 min. (B) FPLC trace of ^{64}Cu-BAT-2IT-1A3-F(ab')$_2$ where the BAT-2IT-1A3-F(ab')$_2$ was purified by FPLC before labeling with ^{64}Cu. The amount of ^{64}Cu-BAT-2IT-1A3-Fab' present decreased significantly. The column calibration with molecular weight markers indicated that 1A3-F(ab')$_2$ fragment (molecular wieght ~100,000 Da) on this FPLC column eluted with a retention time of 34 min.

10%–20% polyacrylamide gradient gels containing 0.1% SDS. Gels were electrophoresed at room temperature at 30 mA per gel. After electrophoresis, gels were fixed and then stained with Serva Blue in 20% methanol. Molecular weight standards and standards of unreacted 1A3-F(ab')$_2$ were electrophoresed in control lanes.

Animal Models

Animal biodistribution experiments were carried out in 6-wk-old immunocompetent male Golden Syrian hamsters implanted with GW39 human colon carcinoma in the musculature of their right thigh (*19*). GW39 tumors express the antigen recognized by MAb 1A3 (*20*). Biodistribution studies were also carried out in normal Sprague-Dawley rats as previously described (*13*).

Biodistributions of ^{64}Cu-benzyl-TETA-1A3-F(ab')$_2$ for dosimetry calculations were determined in mature, female, adult Sprague Dawley rats with weights of 165 ± 10.3 g. The amount of 1A3-F(ab')$_2$ injected per rat ranged from 25–50 μg with a specific activity of 1–2 μCi/μg. Rats were sacrificed at several time points ranging from 1 hr to 36 hr postinjection. Samples of blood and 10 organs were were removed, weighed, counted, and the %ID/g and %ID/organ were calculated for these organs. The assumption was made that the rat biodistribution, which determined %ID/organ at various time points postinjection, is the same as the human biodistribution. Physical decay was assumed for activity remaining in organs beyond 36 hr postinjection. The μCi/organ/mCi values were decay-corrected and plotted versus time. For each organ, the number of μCi-hr/organ/mCi were determined by measuring the area under the curves. For these calculations, it is assumed there is no excretion. The remaining μCi-hr quantity not accounted for by the organs removed was considered to be uniformly distributed in "other" tissue. Dose estimates were then calculated using standard MIRD techniques (*21*).

A 35-kg adult male baboon was repeatedly imaged in a Siemens/CTI ECAT EXACT PET system (CTI PET Systems, Knoxville, TN) to determine the biodistribution of ^{64}Cu-benzyl-TETA-1A3-F(ab')$_2$. The baboon was injected on two occasions with 1 mg of FPLC-purified BAT-2IT-F(ab')$_2$, labeled with 6 and 9.3 mCi of ^{64}Cu, respectively. Images of the animal's torso were acquired at 0, 6, 14 and 38 hr postinjection. The same baboon was injected once with 1 mg of ^{64}Cu-labeled unpurified F(ab')$_2$ and imaged at 2, 8 and 31 hr postinjection.

Activity concentration values were derived from the PET images which had been previously calibrated against the Capintec dose calibrator used to assay the injected doses. Regions of interest (ROIs) drawn over the liver, kidneys and left ventricle were used to estimate total organ and blood-pool accumulations of the compound. Blood activity was taken to be the average of the

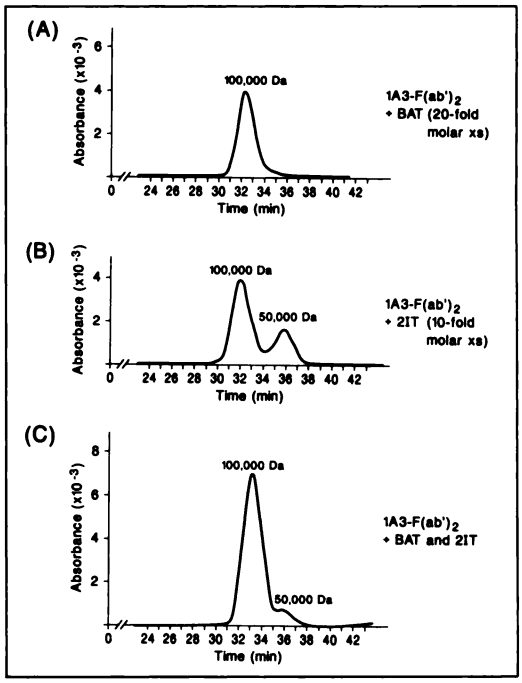

FIGURE 2. FPLC traces of 1A3-F(ab')$_2$ after incubation with BAT, 2IT, or a mixture of BAT and 2IT. (A) FPLC trace of 1A3-F(ab')$_2$ incubated with a 20-fold molar excess of BAT. (B) FPLC trace of 1A3-F(ab')$_2$ incubated with a 10-fold molar excess of 2IT. (C) FPLC trace of 1A3-F(ab')$_2$ incubated with a 20-fold molar excess of BAT and a 10-fold molar excess of 2IT.

TABLE 1
Immunoreactivity and Human Kidney Self-Dose Measurements of ^{64}Cu-BAT-2IT-1A3-F(ab')$_2$ at Different BAT-to-MAb Ratios

BAT:MAb	FPLC Purified	Dose mGy/MBq (rads/mCi)	IR
10:1	No	1.07 (3.97)	77 (n = 1)
10:1	Yes	0.837 (3.10)	85.8 ± 3.2 (n = 3)
20:1	No	1.27 (4.69)	70.0 ± 4.0 (n = 3)
20:1	Yes	0.805 (2.98)	86.9 ± 4.2 (n = 8)

The dose measurements were estimated from rat biodistribution data. The number of IR measurements is given in parentheses next to the value. The IRs of ^{64}Cu-labeled 20:1 FPLC and ^{64}Cu-labeled 20:1 unpurified fragments are significantly different ($p < 0.0005$).

maximum pixels in 5 to 6 adjacent slices. This was necessary to avoid partial volume effects in the moving heart. Liver activity was taken as the average value in a large ROI centered in the liver and averaged over 5 to 6 slices. Kidney activity, although trapped primarily in the renal cortex, was taken as the average value inside an ROI outlining the entire kidney and was assumed to be uniformly distributed in the organ. ROI values were decay-corrected to the time of injection, multiplied by standard human organ volumes normalized to the baboon's weight (*22*), corrected for blood content, and compared with the total injected activity to determine percent injected dose (%ID) to each organ. A 1900-ml blood volume for the baboon was selected to give 100% ID in the blood at time 0. Bone marrow activity was derived from blood pool activity according to the model of Siegel et al. (*23*) using a partition fraction of 0.3.

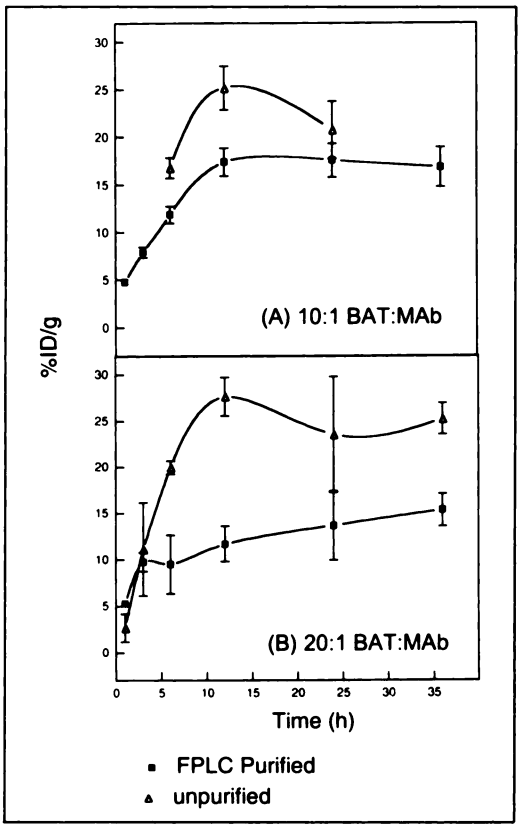

FIGURE 3. Kidney clearance of ^{64}Cu-labeled FPLC-purified and unpurified BAT-2IT-1A3-F(ab')$_2$ in normal Sprague-Dawley rats. (A) 10:1 BAT-to-MAb ratio (FPLC purified, n = 8; unpurified, n = 4); (B) 20:1 BAT-to-MAb ratio (FPLC purified, n = 8; unpurified, n = 4).

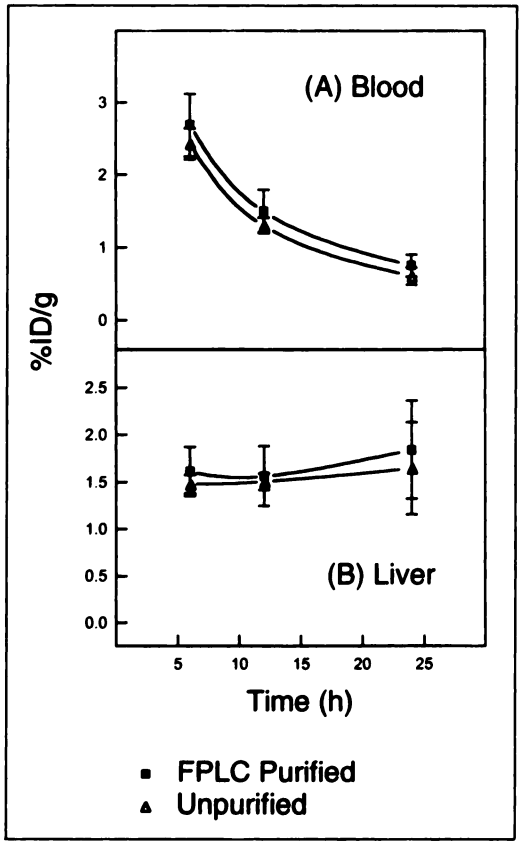

FIGURE 4. Blood and liver clearance of ^{64}Cu-labeled FPLC purified and unpurified BAT-2IT-1A3-F(ab')$_2$ in normal Sprague-Dawley rats. Both conjugates were prepared using a 20:1 BAT-to-MAb molar ratio (FPLC purified, n = 8; unpurified, n = 4).

RESULTS

Preparation of MAb Fragment Conjugates

The MAb 1A3-F(ab')$_2$ fragments were conjugated with BAT at molar ratios of 6:1, 10:1 and 20:1, using a 3:1, 5:1 and 10:1 molar ratio of the linking agent 2IT:MAb, respectively. FPLC analysis of the 10:1 and 20:1 BAT:MAb conjugates showed that 15%–35% was a 50-kD impurity, whereas the 6:1 BAT:MAb conjugate contained approximately 10% of this lower molecular wieght impurity. To eliminate this impurity, BAT-2IT-1A3-F(ab')$_2$ was purified by FPLC following conjugation. FPLC chromatograms of ^{64}Cu-labeled purified and unpurified BAT-2IT-1A3-F(ab')$_2$ are shown in Figure 1. The lower molecular wieght impurity is removed by the FPLC purification, and quality control by FPLC of the radiolabeled FPLC purified conjugate indicates one radioactive product with a molecular wieght of 100,000.

To determine the source of the impurity, 1A3-F(ab')$_2$ was incubated with BAT and 2IT separately and together

and the mixtures were analyzed by FPLC. The FPLC chromatograms shown in Figure 2 indicate that the 2IT caused the impurity. BAT alone did not appear to damage 1A3-F(ab')$_2$. The 50-kD impurity was isolated by FPLC and labeled with ^{64}Cu. The IR of this ^{64}Cu-labeled 50-kD impurity was 28%, and SDS-PAGE showed the 50-kD molecular wieght impurity to co-migrate with 1A3-Fab' fragment (not shown).

The isotopic dilution assay showed that the 20:1 BAT-to-MAb conjugates had two chelates/fragment, whereas the 10:1 conjugates had 1 chelate/fragment and the 6:1 conjugates had less than 0.5 chelates/fragment. Because of the low number of chelates conjugated to 1A3-F(ab')$_2$, ^{64}Cu-labeled conjugates of 6:1 BAT-to-MAb, either with or without FPLC purification, had significantly decreased labeling efficiency compared to the 20:1 and 10:1 BAT-to-MAb conjugates. For this reason, only the 10:1 and 20:1 conjugates were further evaluated. Table 1 shows that FPLC purification of the 10:1 and 20:1 conjugates resulted in improved IR. The greatest improvement in IR was between the ^{64}Cu-labeled FPLC-purified and unpurified 20:1 BAT-to-MAb conjugates (86.9% ± 4.2% versus 70.0% ± 4.0%; $p < 0.0005$). Although the IR results were similar between FPLC-purified 10:1 and 20:1 BAT-to-MAb, the higher BAT-to-MAb resulted in the addition of more chelates which gave a higher radiolabeling efficiency. Thus, the 20:1 BAT-to-MAb conjugate was evaluated more extensively in both animal models.

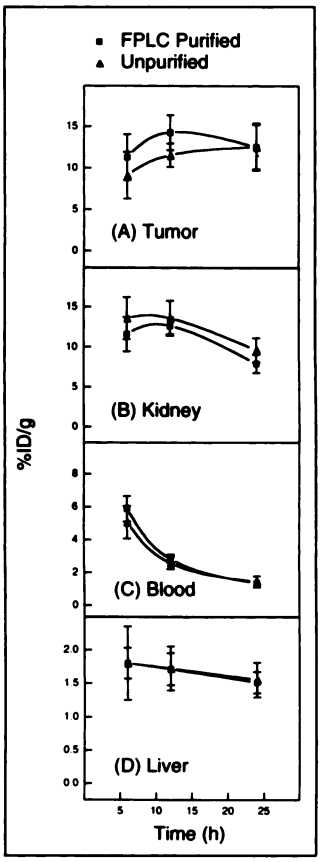

FIGURE 5. Biodistribution of ^{64}Cu-labeled FPLC-purified (n = 12) and unpurified (n = 9) BAT-2IT-1A3-F(ab')$_2$ in tumor-bearing Golden Syrian Hamsters. Statistically significant differences (p values) between uptake of ^{64}Cu-labeled purified and unpurified conjugates are given for each organ. (A) Tumor uptake; 12 hr, p = 0.0034; (B) kidney clearance; 24 hr, p = 0.011 (C) blood clearance; 6 hr, p = 0.044 (D) liver clearance.

Animal Biodistribution

Rat biodistribution experiments were performed using 10:1 and 20:1 BAT-to-MAb conjugates that were prepared with and without FPLC purification. A comparison of the %ID/g of these conjugates in the kidney from 1 to 36 hr postinjection is shown in Figure 3. At both BAT-to-MAb ratios, the conjugates that were not FPLC-purified had significantly higher uptake in the kidneys over time ($p < 0.005$) than the conjugates that were FPLC-purified except for the 10:1 BAT-to-MAb at 24 hr ($p = 0.054$). The highest kidney uptake occurred with unpurified ^{64}Cu-labeled conjugates at 20:1 BAT-to-MAb, most likely because of the greater amount of BAT-2IT-1A3-Fab' formed due to the higher 2IT concentration. Copper-64-BAT-2IT-1A3-Fab', with a molecular wieght of approximately 50 kD, should clear primarily through the kidneys. A comparison of the liver uptake and blood clearance in normal rats shows no significant differences between purified and unpurified ^{64}Cu-labeled 20:1 BAT-to-MAb conjugates (Fig. 4).

Biodistribution experiments were carried out with ^{64}Cu-labeled 20:1 BAT-to-MAb conjugates, both FPLC and non-FPLC purified, using the hamster, GW39 human colon cancer model. Figure 5 shows that the ^{64}Cu-labeled FPLC-purified conjugate demonstrated greater tumor uptake and lower kidney uptake at all three time points compared to the unpurified conjugate, however, the differences were not as pronounced as those observed in normal rats. As in normal rats, there were no significant differences in the blood clearance and liver uptake of the two compounds.

Dosimetry

The human radiation absorbed doses to the kidneys for 10:1 and 20:1 BAT-to-MAb conjugates were calculated from rat biodistribution data and are listed in Table 1. The kidney doses for the ^{64}Cu-labeled FPLC-purified conjugates are significantly lower than those of the radiolabeled

TABLE 2
Absorbed Radiation Doses Resulting from Administration of ^{64}Cu-labeled 20:1 FPLC-Purified BAT-2IT-1A3-F(ab')$_2$ Determined from Normal Rat Biodistribution Data*

Organ	mGy/MBq (Rad/mCi)	mGy/185 MBq (Rad/5 mCi)
Kidneys	0.805 (2.98)	149 (14.9)
Liver	0.123 (0.455)	22.8 (2.28)
Marrow	0.107 (0.395)	19.8 (1.98)
Spleen	0.101 (0.373)	18.7 (1.87)
ULI wall	0.117 (0.432)	21.6 (2.16)
Small intestine	0.067 (0.247)	12.4 (1.24)
Stomach wall	0.043 (0.158)	7.90 (0.790)
LLI wall	0.212 (0.786)	39.3 (3.93)
Lungs	0.037 (0.138)	6.90 (0.690)
Other	0.022 (0.082)	4.10 (0.410)
Total body	0.031 (0.115)	5.75 (0.575)

*The effective dose is 0.14 mSv MBq^{-1} (0.516 rem/mCi).

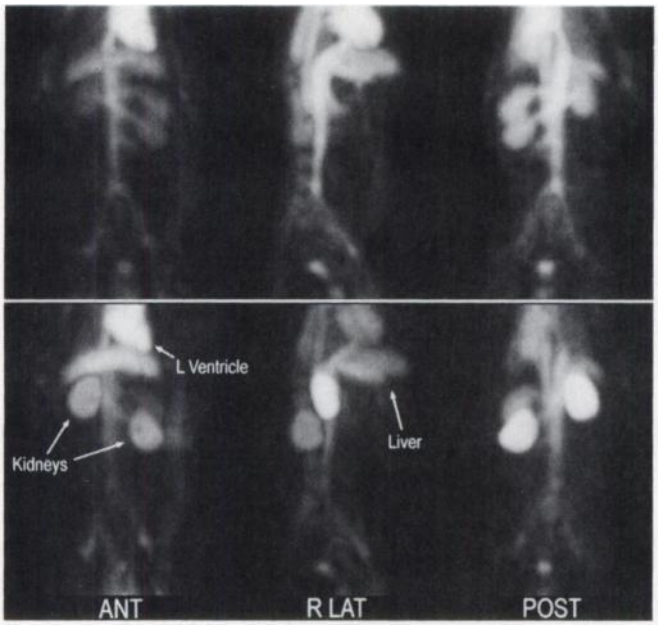

FIGURE 6. Reprojected PET torso images of baboon following injection of 9.3 mCi ^{64}Cu-BAT-2IT-1A3-F(ab')$_2$ (FPLC purified). Top images show the biodistribution of the compound in the first hour following injection, while the bottom images were taken 6–7 hr postinjection. Images are self-normalized; however, substantial accumulation in the kidneys and decreasing blood-pool activity are evident.

unpurified conjugates. The ^{64}Cu-labeled unpurified 20:1 BAT-to-MAb conjugate gave the highest dose to the kidney (1.27 mGy/MBq) which correlates with the greatest amount of ^{64}Cu-BAT-2IT-1A3-Fab' injected. Table 2 lists the absorbed radiation dose of ^{64}Cu-BAT-2IT-1A3-F(ab')$_2$ (20:1 BAT-to-MAb, FPLC-purified conjugate) for nine organs as well as the total body. The kidney was the critical organ (0.805 mGy/MBq), followed by the lower large intestine wall (LLI) (0.212 mGy/MBq), the liver (0.123 mGy/MBq) and the upper large intestine wall (ULI) (0.117 mGy/MBq). Also listed in Table 2 are the corresponding absorbed doses for a 185-MBq injection, a likely imaging dose for clinical studies.

Human absorbed doses to the kidneys for both ^{64}Cu-labeled FPLC and unpurified fragments were also calculated from PET images of a baboon (Fig. 6). Time-activity curves (TAC) for the kidneys constructed from these data are shown in Figure 7A plotting %ID versus time after injection. Figure 7B shows the TAC for the blood clearance. A least-squares fit of each data set is also shown. To use the MIRD scheme, a quantity known as the "residence time," which is the accumulation-time product, is determined for each organ by integrating the analytical form of the TAC from 0 to ∞. Residence times for blood pool, liver and kidneys were determined for the baboon, thereby accounting for 60%–85% of the injected activity over the imaging period. These values were assumed to be predictive of the pharmacokinetics in a human. By visual assessment, no other substantial accumulation was evident in the animal, and the missing fraction, increasing from 15%–40%, was determined to be distributed uniformly in the soft tissue. A "remainder of body" compartment was used in the dosimetry model to account for blood activity and any missing activity. The liver, kidneys, red bone marrow and remainder of body were then used as source organs in the MIRD scheme to estimate the total dose to each organ in mGy/MBq injected. Results of the absorbed doses calculations for the liver and kidneys are shown in Table 3.

DISCUSSION

Copper-64, a positron-emitting isotope with a 12.8-hr $T_{1/2}$, has many advantages for tumor imaging when labeled to MAbs. Copper-64 is readily available from MURR in high specific activity and is less expensive than many cyclotron-produced isotopes. It has been shown that PET imaging with ^{64}Cu-BAT-2IT-1A3 is more sensitive for smaller metastatic lesions than ^{111}In-labeled 1A3-F(ab')$_2$ using the bifunctional chelate *N,N'-bis*(2-hydroxybenzyl)-1-(4-bromoacetamidobenzyl)-1,2-ethylenediamine-*N,N'*-diacetic acid (BrΦHBED) (*1*). Copper-64 also has possible applications in therapy, as it has been shown to have similar lethality to ^{67}Cu in vitro, both when uncomplexed or labeled to MAb 1A3 (*24–26*).

Copper-64-BAT-2IT-1A3-F(ab')$_2$ has advantages over ^{64}Cu-labeled intact 1A3 which include a shorter biological half-life, lower liver uptake and potentially decreased HAMA response. The tumor-to-nontumor ratios of ^{64}Cu-BAT-2IT-1A3-F(ab')$_2$ were better than those for ^{111}In-BrΦHBED-1A3-F(ab')$_2$ and except for the tumor-to-kidney ratio, comparable or better than ^{125}I-1A3-F(ab')$_2$ (*13*). The major problem with ^{64}Cu-BAT-2IT-1A3-F(ab')$_2$ in these studies was the high kidney uptake which was caused in part by a 50-kD impurity. FPLC and SDS-PAGE analysis showed this impurity to be ^{64}Cu-BAT-2IT-1A3-Fab'. This fragment had low immunoreactivity (28%), and because of its size, it most likely cleared primarily through the kidneys. BAT-2IT-1A3-Fab' was produced during conjugation as a result of partial reduction of 1A3-F(ab')$_2$ interchain disulfide bonds by 2IT (Fig. 2). The BAT-2IT-1A3-F(ab')$_2$ was purified from the BAT-2IT-1A3-Fab' impurity using FPLC. Because FPLC purification is time-consuming, various BAT-to-MAb ratios with corresponding decreasing amounts of 2IT were investigated in hopes of decreasing the production of BAT-2IT-1A3-Fab' and eliminating the FPLC purification step. Even at the lowest BAT-to-MAb ratio investigated (6:1), there was sufficient BAT-2IT-1A3-Fab' contamination, necessitating FPLC purification. At 6:1 BAT-to-MAb, for every two molecules of 1A3-F(ab')$_2$, only one was conjugated with BAT. This compromised labeling efficiency to such an extent that we chose not to further investigate this conjugate. When labeled with ^{64}Cu, the 20:1 conjugate had twice the labeling efficiency of the 10:1 conjugate. There were no major differences in the kidney uptake of ^{64}Cu-labeled FPLC-purified conjugates using 10:1 and 20:1 BAT-to-MAb ratios. Based on these data, the optimum BAT-to-MAb ratio for

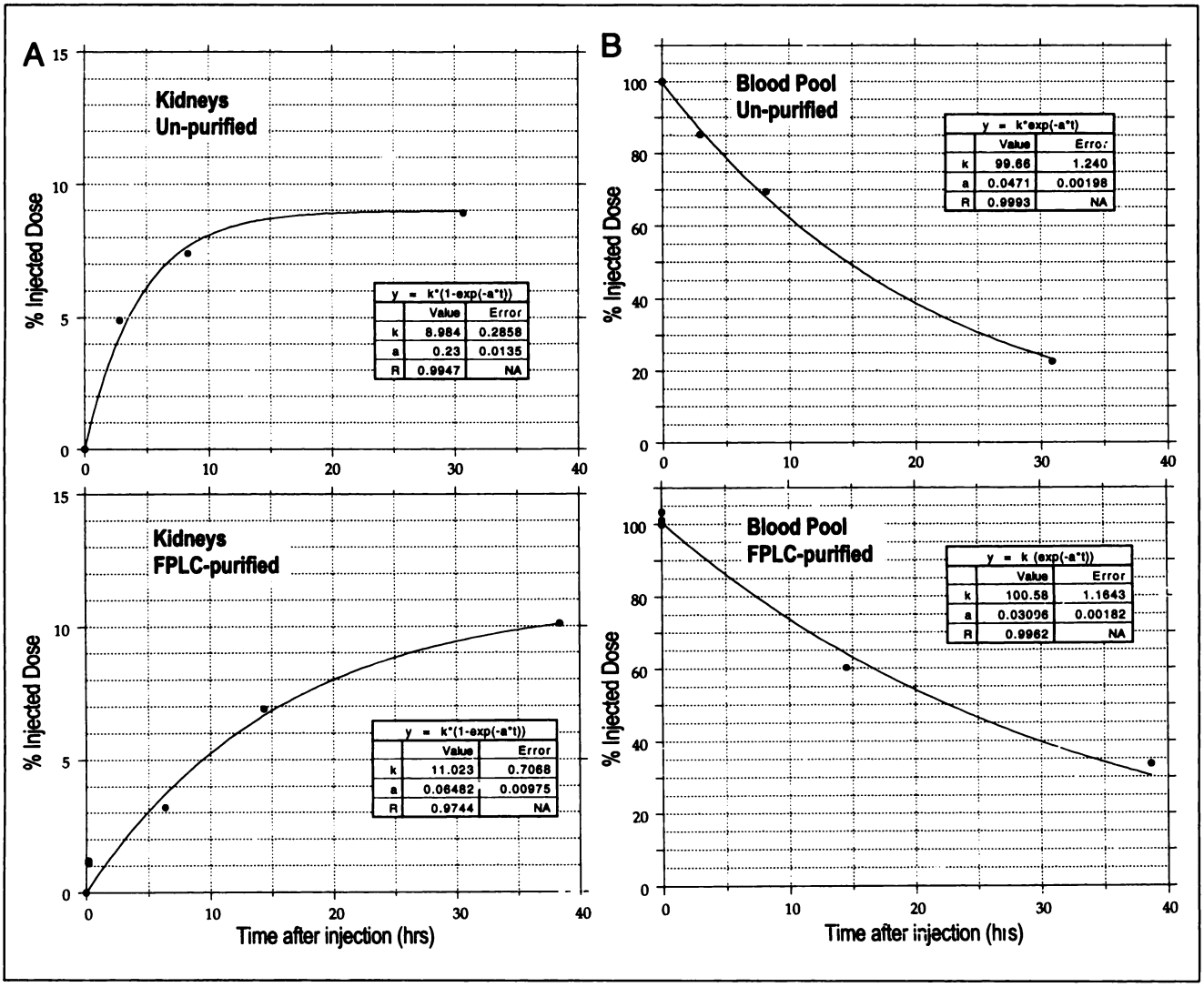

FIGURE 7. Time-activity curves for (A) kidneys and (B) blood from PET images of a baboon injected with ^{64}Cu-labeled FPLC purified BAT-2IT-1A3-F(ab')$_2$ (top) or ^{4}Cu-labeled unpurified BAT-2IT-1A3-F(ab')$_2$ (bottom).

achieving acceptable labeling efficiency and kidney clearance was 20:1 with FPLC purification.

Although the differences in kidney uptake in tumor-bearing hamsters between ^{64}Cu-labeled FPLC-purified and unpurified conjugates were not as dramatic as in normal rats, the same trends were observed, and FPLC purification decreased kidney uptake. It is interesting to note that the kidney uptake of both ^{64}Cu-labeled FPLC-purified and unpurified conjugates in the hamsters clear significantly after 12 hr postinjection, whereas in the rats, only the 10:1 ^{64}Cu-labeled unpurified conjugates showed any clearance. At this time, we have no explanation for the differences between the two animal models.

In hamsters, the ^{64}Cu-labeled FPLC-purified BAT-2IT-1A3-F(ab')$_2$ had a higher tumor uptake at 6 and 12 hr postinjection, most likely due to the higher IR. It was expected that the presence of a 50-kD impurity in the unpurified conjugate might increase the rate of blood clearance, as well as decrease the amount of activity in the liver;

TABLE 3
Absorbed Radiation Doses Resulting from Administration of ^{64}Cu-Labeled 20:1 Unpurified and FPLC-Purified BAT-2IT-1A3-F(ab')$_2$ Determined from PET Imaging of a Normal Baboon

Organ	Unpurified mGy/MBq (rad/mCi)	FPLC Purified mGy/MBq (rad/mCi)
Kidneys	0.385 (1.42)	0.309 (1.14)
Liver	0.120 (0.444)	0.140 (0.517)
Marrow	0.041 (0.150)	0.048 (0.176)
Spleen	0.032 (0.118)	0.031 (0.114)
ULI wall	0.031 (0.115)	0.031 (0.115)
Small intestine	0.031 (0.114)	0.031 (0.113)
Stomach wall	0.030 (0.111)	0.030 (0.109)
LLI wall	0.029 (0.108)	0.029 (0.107)
Lungs	0.028 (0.102)	0.028 (0.102)
Other	0.027 (0.098)	0.026 (0.097)
Total body	0.031 (0.114)	0.031 (0.114)

however, the blood clearance and liver uptake were similar between the two compounds in both animal models.

There are few reports of Cu-labeled MAb fragments in the literature. In one recent study, ^{67}Cu was labeled to MAb35 F(ab')$_2$, an anti-colon carcinoma MAb F(ab')$_2$ using the macrocyclic bifunctional chelate 4-(1,4,8,11-tetraazacyclotetradec-1-yl)methylbenzoic acid (14N4 (*27*), also called CPTA (*28*)). The authors concluded that the high kidney uptake (36.7% ± 4.98% ID/g at 12 hr postinjection) precludes the clinical use of ^{67}Cu-labeled MAb35 F(ab')$_2$ for therapy studies. A recent in vivo comparison of the bifunctional chelates CPTA and BAT conjugated to 1A3-F(ab')$_2$ showed ^{64}Cu-CPTA-1A3-F(ab')$_2$ to have a significantly higher kidney uptake than ^{64}Cu-BAT-2IT-1A3-F(ab')$_2$ (27.6% ± 2.25% ID/g and 13.66% ± 3.71% ID/g, respectively, at 24 hr postinjection ($p < 0.001$)) (*29*). The conjugation of CPTA to 1A3-F(ab')$_2$ did not cause the breakage of disulfide bonds forming 1A3-Fab' (Anderson CJ, *unpublished results*); therefore, the higher kidney uptake could not be attributed to radiolabeled, lower molecular wieght fragments. This large difference in kidney uptake may indicate that the metabolite of ^{64}Cu-BAT-2IT-1A3-F(ab')$_2$ is released from kidney cells more readily than that of ^{64}Cu-CPTA-1A3-F(ab')$_2$. Another possible explanation is that the ^{64}Cu-CPTA chelate was unstable in the kidneys and free $^{64}Cu^{2+}$ bound to intracellular proteins in the kidneys, trapping the ^{64}Cu in the kidneys. The significant differences in kidney uptake between ^{64}Cu-BAT-2IT-1A3-F(ab')$_2$ and ^{64}Cu-CPTA-1A3-F(ab')$_2$, which differ only in the chelate and chelate-MAb linkage, suggest that a better understanding of the metabolism of radiolabeled chelate-MAb conjugates may aid in the design of bioconjugate radiopharmaceuticals that more rapidly clear nontarget organs. Studies to better understand the metabolism of ^{64}Cu-labeled immunoconjugates are ongoing.

The estimated human absorbed doses for FPLC-purified (20:1) ^{64}Cu-BAT-2IT-1A3-F(ab')$_2$ based on biodistribution data in Sprague-Dawley rats are listed in Table 2 for nine organs and for the total body. These dose estimates are conservative since no excretion is assumed. No extrapolation method has been used to fit the animal data to man, since no method has been recognized to be more accurate than direct application of animal organ residence times to man (*10,30*). In our study, primary and secondary critical organs have been identified as the kidneys (0.805 mGy/MBq) and lower large intestine (0.212 mGy/MBq). The absorbed doses to the bone marrow, spleen and total body were estimated to be 0.107, 0.101 and 0.031 mGy/MBq. These doses are within an acceptable range for clinical use. The effective dose equivalent (EDE) for FPLC-purified ^{64}Cu-BAT-2IT-1A3-F(ab')$_2$ is 0.14 mSv MBq^{-1}, and for a clinical dose of 185 MBq, the EDE would be 25.9 mSv (*31*).

Based on rat biodistribution data, we previously reported an absorbed dose estimate to the kidneys for ^{64}Cu-labeled unpurified BAT-2IT-1A3-F(ab')$_2$ to be 1.1 mGy/MBq (*13*). A recalculated value, 1.27 mGy/MBq, has accounted for physical decay beyond the 36-hr biodistribution study. FPLC purification of BAT-2IT-1A3-F(ab')$_2$ caused a 36% decrease in the kidney absorbed dose from 1.27 mGy/MBq to 0.805 mGy/MBq. The reduction in kidney uptake for the ^{64}Cu-labeled FPLC-purified conjugate was noted as early as 6 hr postinjection and remained significantly lower up to 36 hr, decreasing the overall residence time in the kidney. From these dosimetry estimates, an injected dose of 185 MBq will result in a kidney absorbed dose of 149 mGy.

The absorbed doses to the kidneys were also determined for both ^{64}Cu-labeled FPLC-purified and unpurified BAT-2IT-1A3-F(ab')$_2$ from PET images of a normal baboon. A comparison of the dose estimates to the kidneys shows a 22% reduction for the ^{64}Cu-labeled FPLC-purified conjugate. The blood clearance for the ^{64}Cu-labeled unpurified conjugate was more rapid than that of the FPLC-purified. These differences support our conclusion that the lower molecular wieght impurity is cleared from the blood more rapidly by the kidneys, where it is trapped, thereby increasing the kidney dose. The difference is not significant for the $n = 1$ study we have performed here, however, the trend is in the same direction as that seen in the rat biodistribution.

The absorbed dose to the kidneys based on rat biodistribution (showing ~25% ID in the kidneys) was 0.81 mGy/MBq for ^{64}Cu-labeled purified conjugate. Alternatively, baboon PET image data showed only ~10% ID in the kidneys and an absorbed dose of 0.31 mGy/MBq. The different biodistribution between nonhuman primates and rodents is not surprising, given that hepatobiliary and renal clearance of many radiopharmaceuticals varies widely from rodents to mammals (*32,33*). The differing dosimetry results obtained in rodents versus a primate raises questions concerning the use of rodents to determine human dose estimates. Given the expense and scarcity of primates for use in research studies, rodents provide a conservative estimate of human absorbed doses for initiating clinical trials for new radiopharmaceuticals. Based on the dosimetry from the baboon PET image, an injected dose of 185 MBq will result in a total dose to the kidneys of 56.8 mGy for ^{64}Cu-labeled purified BAT-2IT-1A3-F(ab')$_2$, whereas the kidney dose based on rat biodistribution studies is 149 mGy. This dose is significant, but still at or below the primary critical organ dose for several FDA-approved radiopharmaceuticals routinely used in nuclear medicine such as ^{111}In-WBC, 200 mGy to the spleen (package insert, ^{111}In-oxine, Amersham Healthcare); Oncoscint®, 150 mGy to the spleen, 90 mGy to the liver (package insert, Cytogen, Inc.); and Octreoscan®, 148 mGy to the spleen (package insert, Mallinckrodt Medical, Inc.).

CONCLUSION

This paper describes the optimization of the preparation of ^{64}Cu-BAT-2IT-1A3-F(ab')$_2$, which gives improved biodistribution in three animal models. FPLC purification of the BAT-2IT-1A3-F(ab')$_2$ conjugates eliminated a 50-kD

impurity, believed to be BAT-2IT-1A3-Fab′, resulting from the reduction of disulfide bonds by the linking agent 2IT. The ^{64}Cu-labeled FPLC-purified conjugates showed significantly increased immunoreactivity and decreased kidney uptake in Sprague-Dawley rats over that of the ^{64}Cu-labeled unpurified conjugates. By using the FPLC purification procedure, the estimated human absorbed dose to the kidneys of ^{64}Cu-BAT-2IT-1A3-F(ab′)$_2$ decreased from 1.27 to 0.805 mGy/MBq based on rat biodistribution data, while data from a primate PET imaging study showed kidney uptake decreasing from 0.38 to 0.31 mGy/MBq. With the kidney as the critical organ, 185 MBq of ^{64}Cu-BAT-2IT-1A3-F(ab′)$_2$ can be administered clinically with reasonable absorbed doses.

ACKNOWLEDGMENTS

The authors thank Pamela A. Rocque, Henry V. Lee and Elizabeth L.C. Sherman for their excellent technical assistance. This work was supported by NIH grant CA44728 (GWP) and DOE grant DE-FG02-87-ER60512 (MJW).

REFERENCES

1. Philpott GW, Schwarz SW, Anderson CJ, et al. Initial clinical study of Cu-64-labeled anticolon-carcinoma monoclonal antibody (MAb 1A3) in colorectal cancer [Abstract]. *J Nucl Med* 1993;34:81P.
2. Philpott GW, Dehdashti F, Schwarz SW et al. Positron emission tomography (PET) with Cu-64-labeled monoclonal antibody (MAb 1A3) in colorectal cancer [Abstract]. *J Nucl Med* 1994;35:12P.
3. Keenan AM, Harbart JC, Larson SM. Monoclonal antibodies in nuclear medicine. *J Nucl Med* 1985;26:531–537.
4. Massuger LFAG, Claessens RAMJ, Pak KY, et al. Tissue distribution of ^{99m}Tc, ^{111}In and ^{123}I-OV-TL 3 Fab′ in ovarian carcinoma bearing nude mice. *Nucl Med Biol* 1991;18:77–83.
5. Wang TST, Fawwaz RA, Alderson PO. Reduced hepatic accumulation of radiolabeled monoclonal antibodies with indium-111-thioethre-poly-L-lysine-DTPA-monoclonal antibody-TP41.2F(ab′)$_2$. *J Nucl Med* 1992;33:570–574.
6. Yemul S, Leon JA, Pozniakoff T, Esser PD, Estabrook A. Radioimmunoimaging of human breast carcinoma xenografts in nude mouse model with ^{111}In-labeled new monoclonal antibody EGA-1 and F(ab′)$_2$ fragments. *Nucl Med Biol* 1993;20:325–335.
7. Kuhlmann L, Steinsträsser A. Effect of DTPA to antibody ratio on chemical, immunological and biological properties of the ^{111}In-labeled F(ab′)$_2$ fragment of the monoclonal antibody 431/31. *Nucl Med Biol* 1988;15:617–627.
8. Yemul S, Leon JA, Seldin DW, Link M-J, Kramer, Mesa-Tejada R, Estabrook A. Tumor localization in nude mice bearing human breast carcinoma xenografts using ^{111}In-DTPA conjugates of monoclonal antibodies. *Nucl Med Biol* 1991;18:295–304.
9. Andrew SM, Perkins AC, Pimm MV et al. A comparison of iodine and indium labeled anti-CEA intact antibody, F(ab′)$_2$ and Fab fragments by imaging tumor xenografts. *Eur J Nucl Med* 1988;13:598–604.
10. Jönsson B-A, Strand S-E, Andersson L. Radiation dosimetry for indium-111-labeled anti-CEA-F(ab′)$_2$ fragments evaluated from tissue distribution in rats. *J Nucl Med* 1992;33:1654–1660.
11. Chetanneau A, Baum RP, Lehur PA, et al. Multi-centre immunoscintigraphy study using indium-111-labeled CEA-specific and/or 19-9 monoclonal antibody F(ab′)$_2$ fragments. *Eur J Nucl Med* 1990;17:223–229.
12. Buccheri G, Biggi A, Ferrigno D, et al. Imaging lung cancer by scintigraphy with indium-111-labeled F(ab′)$_2$ fragments of the anticarcinoembryonic antigen monoclonal antibody FO23C5. *Cancer* 1992;70:749–759.
13. Anderson CJ, Connett JM, Schwarz SW, et al. Copper-64-labeled antibodies for PET imaging. *J Nucl Med* 1992;33:1685–1691.
14. Moi MK, Meares CF, McCall MJ, Cole WC, DeNardo SJ. Copper chelates as probes of biological systems: stable copper complexes with a macrocyclic bifunctional chelating agent. *Anal Biochem* 1985;148:249–253.
15. McCall MJ, Diril H, Meares CF. Simplified method for conjugating macrocyclic bifunctional chelating agents to antibodies via 2-iminothiolane. *Bioconj Chem* 1990;1:222–226.
16. Penefsky HS. A centrifuged column procedure for the measurement of ligand binding by beef heart ATPase. In: Fleischer S, ed. *Methods in enzymology*, vol. 56 part G. New York: Academic Press; 1979:527–530.
17. Zinn KR, Chaudhuri TR, Cheng TP, Meyer WA, Morris JS. Production of no-carrier added ^{64}Cu from zinc metal irradiated under boron shielding. *Cancer* 1994;73:774–778.
18. Lindmo T, Boven E, Cutteta F, Federko J, Bunn PA Jr. Determination of the immunoreactive fraction of radiolabeled monoclonal antibodies by linear extrapolation to binding at infinite antigen excess. *Immunol Meth* 1984;72:77–89.
19. Goldenberg DM, Witte S, Elster K. GW-39: a new human tumor serially transplantable in the golden hamster. *Transplantation* 1967;4:760–763.
20. Fenwick JR, Philpott GW, Connett JM. Biodistribution and histological localization of anti-human colon cancer monoclonal antibody (MAb) 1A3: the influence of administered MAb dose on tumor uptake. *Int J Cancer* 1989;44:1017–1037.
21. *MIRD pamphlet no. 11*. New York: Society of Nuclear Medicine; 1975.
22. Cloutier RJ, Watson EE. Radiation dose from radioisotopes in the blood. *Proceedings of the symposium on medical radionuclides radiation dose and effects*. Oak Ridge Associated Universities; 1970:325–346.
23. Siegel JA, Wessels BW, Watson EE, et al. Bone marrow dosimetry and toxicity for radioimmunotherapy. *Antibody Immunoconj Radiopharm* 1990;3:213–233.
24. Apelgot S, Coppey J, Gaudemer A, et al. Similar lethal effect in mammalian cells for two radioisotopes of copper with different decay schemes, ^{64}Cu and ^{67}Cu. *Int J Radiat Biol* 1989;55:365–384.
25. Anderson CJ, Connett JM, Baumann ML, et al. Comparison of Cu-67 and Cu-64 as potential radionuclides for radiotherapy [Abstract]. *J Nucl Med* 1993;34:134P.
26. Connett JM, Anderson CJ, Baumann ML, et al. Cu-67 and Cu-64-labeled monoclonal antibody (MAb) 1A3 as potential agents for radioimmunotherapy [Abstract]. *J Nucl Med* 1993;34:216P.
27. Smith A, Alberto R, Blaeuenstein P, Novak-Hofer I, Maecke HR, Schubiger PA. Preclinical evaluation of ^{67}Cu-labeled intact and fragmented anti-colon carcinoma monoclonal antibody MAb35. *Cancer Res* 1993;53:5727–5733.
28. Smith-Jones PM, Fridrich R, Kaden TA, et al. Antibody labeling with copper-67 using the bifunctional macrocycle 4-[(1,4,8,11-tetraazacyclotetradec-1-yl-methyl]benzoic acid. *Bioconj Chem* 1991;2:415–421.
29. Anderson CJ, Rogers BE, Connett JM, et al. Comparison of two bifunctional chelates for labeling ^{64}Cu to MAb 1A3 and 1A3-F(ab′)$_2$: chemistry and animal biodistribution. *J Lab Compd Radiopharm* 1994;35:313–315.
30. Roedler HD. Accuracy of internal dose calculations with special consideration of radiopharmaceutical biokinetics. In: Watson EE, Schlafke-Stelson AT, Coffey JL, Cloutier RJ, eds. *Third International Radiopharmaceutical Dose Symposium, October 7–10, 1980*; Oak Ridge, TN/Washington, DC: US Department of Health and Human Services, Bureau of Radiological Health; DHHS Publication FDA 81-8166; 1981:1–20.
31. The International Commission of Radiological Protection. *ICRP Publication 26*; 1977.
32. Fritzberg AR, Bloedow DC. Animal models in the study of hepatobiliary radiotracers. In: Lambrecht RM, Eckelman WC, eds. *Animal models in radiotracer design*. New York: Springer Verlag; 1983:179–209.
33. McAfee JG, Subramanian G. Experimental models and evaluation of animal data for renal radiodiagnostic agents. In: Lambrecht RM, Eckelman WC, eds. *Animal models in radiotracer design*. New York: Springer Verlag; 1983:211–227.